Article

Optimal Sizing of a Stand-Alone Hybrid Power System Based on Battery/Hydrogen with an Improved Ant Colony Optimization

Weiqiang Dong [1,2], Yanjun Li [1,]* and Ji Xiang [3]

[1]   School of Information and Electrical Engineering, Zhejiang University City College, Hangzhou 310015, Zhejiang, China; dongwq0911@zju.edu.cn
[2]   College of Control Science and Engineering, Zhejiang University, Hangzhou 310027, Zhejiang, China
[3]   College of Electrical Engineering, Zhejiang University, Hangzhou 310027, Zhejiang, China; jxiang@zju.edu.cn
[*]   Correspondence: liyanjun@zucc.edu.cn; Tel.: +86-571-8828-5727

Abstract: A distributed power system with renewable energy sources is very popular in recent years due to the rapid depletion of conventional sources of energy. Reasonable sizing for such power systems could improve the power supply reliability and reduce the annual system cost. The goal of this work is to optimize the size of a stand-alone hybrid photovoltaic (PV)/wind turbine (WT)/battery (B)/hydrogen system (a hybrid system based on battery and hydrogen (HS-BH)) for reliable and economic supply. Two objectives that take the minimum annual system cost and maximum system reliability described as the loss of power supply probability (LPSP) have been addressed for sizing HS-BH from a more comprehensive perspective, considering the basic demand of load, the profit from hydrogen, which is produced by HS-BH, and an effective energy storage strategy. An improved ant colony optimization (ACO) algorithm has been presented to solve the sizing problem of HS-BH. Finally, a simulation experiment has been done to demonstrate the developed results, in which some comparisons have been done to emphasize the advantage of HS-BH with the aid of data from an island of Zhejiang, China.

Keywords: hybrid system based on battery and hydrogen (HS-BH); hydrogen storage subsystem; ant colony optimization (ACO); annual system cost; loss of power supply probability (LPSP)

1. Introduction

Fossil fuel resources are becoming scarce because of ever-increasing energy demand in commercial, industrial, agricultural and domestic sectors, etc. [1]. In this context, alternative energy resources, like solar, wind, hydro, biomass and geothermal, are being utilized largely to generate power in recent years [2,3]. A distributed power system in which one or more energy sources are utilized could work in grid mode or island mode [4,5]. Owing to seasonal and periodical variations, a hybrid power system including more than one kind of renewable energy source is more reliable than a single-renewable energy power system when providing load supply [6]. Usually, a hybrid power system is built for these situations, which are far away from the power grid, like border posts, islands, hills, and so on. A reliable sizing for the hybrid power system could make each component work at full capacity when converting energy into other types. Additionally, it is very significant because of improving the power supply reliability and reducing the annual system cost. The main work of our paper was carried out from the following three aspects:

(a)　System description: In the past few years, there has been growing interest/concern about the sizing of hybrid power systems [7–11]. In [7,8], the authors have addressed the optimal sizing and scheduling of an isolated wind/photovoltaic (PV) system with battery storage and have presented the results of investigations for meeting the annual load and minimizing the total annual cost to the customer. In [9], Akella and Sharma have studied the sizing of an integrated renewable energy system (IRES) consisting of micro hydrogen power, PV panels and a wind turbine and have reported the results of the optimization of IRES models of the study area of Zone 4 of Jaunpur block of Uttaranchal state. In [10], Elbaset has constructed a PV/fuel cell (FC) hybrid power generation system and presented a computer program to size the system components in order to match the load, for high operational reliability with respect to the objective-loss of power supply probability (LPSP). In [11], Vafaei and Mehdi have developed a microgrid for a remote community in northern Ontario (Canada) that combines wind, as a renewable source of energy, and a hydrogen-based energy storage system was developed with the goal of meeting the demand, while minimizing the cost of energy and adverse effect on the environment. However, most of these studies only contain a single storage unit or a single renewable energy source. A single storage device is easy to dispose of, but it has disadvantages. For example, the battery is efficient to release and store electrical energy, but it is expensive and has an innate leakage characteristic. The efficiency of a hydrogen subsystem consisting of FC, hydrogen tanks and electrical is lower than a battery; but, the subsystem is somehow less expensive, and hydrogen could be left for a long time [12].

Few research works have been done in hybrid systems with both multi-generation units and multi-storage units. In this paper, a stand-alone hybrid system based on a battery and hydrogen (HS-BH) is designed. Both the battery and hydrogen subsystem are adopted so as to utilize their advantages and reduce the negative impact of their shortcomings. Due to the complementary nature characteristic of photovoltaic and wind [13], PV/wind turbine (WT) are beneficial to the generation units of HS-BH. The block of such a system is shown in Figure 1, where multi-generation units are connected to a direct current (DC) bus, batteries and hydrogen tanks used as multi-storage units.
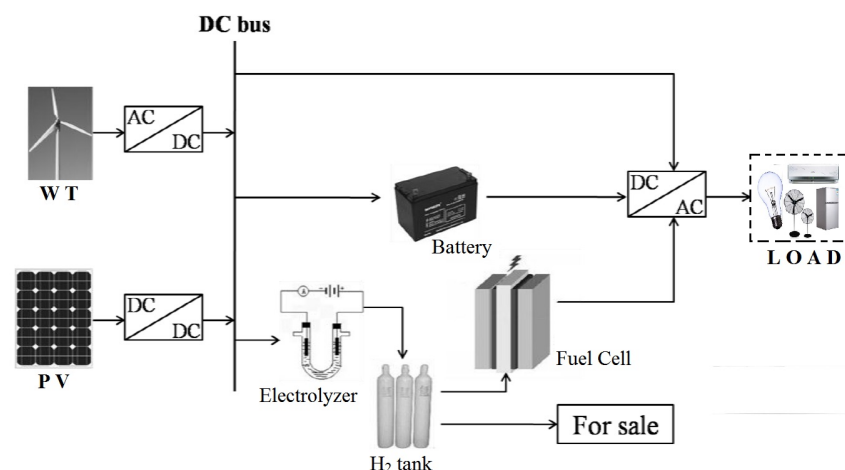

Figure 1. Basic constitution of hybrid system based on battery and hydrogen (HS-BH).

(b)　Objectives design: When sizing for such hybrid power systems, system cost and energy supply reliability are the focus [14–17]. Kashefi et al. have proposed that the most important challenge in the design of a hybrid power system is reliable supply for load demand under various weather situations, considering investment, maintenance and replacement cost. These costs they considered were just caused by the usage of devices, while other costs were ignored.

In this paper, annual system cost is designed from a more comprehensive perspective: not only including devices' cost (DEC), but also including energy waste cost (EWC) and hydrogen profit (HPC). If the available energy of HS-BH is more than the load demand, and it could be stored, EWC will be caused. When checking the status of HS-BH at some time, if there is still hydrogen in the hydrogen subsystem, we could use it in other areas, such as selling. Therefore, HPC could be gained. In fact, EWC and HPC are both related to DEC. Additionally, the LPSP is used for the index of reliability as others' research.

(c) Solving algorithm: Many authors have investigated some classical algorithms for sizing stand-alone hybrid systems based on renewable sources and storage devices [8,18–20]. In [18], a nonlinear programming has been used to find the optimal sizing and location of grid-connected wind turbines based on the simulation of various scenarios. Akella [9], Kellogg and Nehrir [7] and Kuznia et al. [19] have adopted different linear programming models to optimize the design of a hybrid system. In [20], Malheiro and Castro have addressed the sizing and scheduling of hybrid isolated systems via a mixed-integer linear programming. However, classical algorithms could not obtain the global optimal solution within a reasonable amount of time for NP problems. In the last few decades, new generation artificial algorithms, like genetic algorithm (GA) and particle swarm optimization (PSO), were widely used because they required less computation time and had better accuracy [21]. In [22–24], GA has been used for optimal sizing of a hybrid wind/PV/battery power system, which is subject to the reliability index of LPSP. PSO has been successfully implemented for optimal sizing of hybrid stand-alone power systems [25–27]. Furthermore, in [28], a novel approach consisting of a ε-constraint method and PSO has been applied to minimize simultaneously the total cost of the system, unmet load and fuel emission. Besides, a building algorithm that is easily programmable and can be accomplished by a simple search technique has been proposed in [29].

The ant colony algorithm (ACO) has the virtue of simpleness, robustness and being parallel in essence. ACO is efficient in the path routing field as presented in the study by Wang et al. in [30] and the study of Luo and Wu in [31]. In the field of power systems, Carpaneto and Chicco [32] have used ACO to minimize the loss reconfiguration of distribution systems. This work will demonstrate the feasibility and effectiveness of ACO in the sizing of hybrid power systems. In order to improve the efficiency of ACO and avoid falling into local optima, an improved ACO with a real encoding and sorting mechanism is proposed for the sizing of HS-BH.

The contributions of this work are to formulate an HS-BH in the power system sizing problem, considering both the battery and hydrogen subsystem and to design the annual system cost fully consisting of DEC, EWC and HPC. Additionally, the advantage of HS-BH, which contains PV, WT, a battery and a hydrogen subsystem, would be seen in the comparison experiments.

As described above, in the research field of the smart grid, most of the research works on the sizing problem have shown us the PV/battery system, the WT/battery system, the PV/WT/battery system, the PV/WT/FC system, etc.; while in this paper, HS-BH has combined battery and FC that could not only store surplus energy, but also could produce some hydrogen for other purposes, so as to decrease system cost. Furthermore, many former studies considered the DEC only including investment cost, operation and maintenance cost and replacement cost, which will be introduced in a later section. However, in this work, the system cost consisting of DEC, EWC and HPC has been considered more comprehensively. Thus, a satisfactory solution balancing among the system costs, as well as hydrogen profits requires carefully choosing.

Sizing the problem of HS-BH has been solved by an improved ACO, which is based on a real encoding and sorting mechanism, so as to minimize the annual system cost when the limitation of LPSP was given.

The rest of this paper is organized as follows. The problem definition and the model of the hybrid system are given in Section 2, followed by the objectives of this work in Section 3; Section 4 presents

an improved ant colony optimal algorithm, which is adopted for the sizing problem; in Section 5, the simulation data for the optimal sizing is given, with the results being discussed, including comparison simulations. At last, a conclusion for this work is performed.

2. Sizing Formulation

2.1. Problem Description

The goal of this work is to optimize the size of HS-BH for reliable and economic supply, which consists of four subsystems, including photovoltaic, wind energy, batteries and hydrogen energy. Assumed given are the availability of the renewable resources, energy demand profile, as well as the general technical characteristic of commercially available equipment (rated power, efficiency, capital cost, etc.). The objective is the optimal design of the system that minimizes the annual system cost, which consists of DEC, EWC and HPC, and maximizes the reliability, described as LPSP, while meeting energy demand. Note that batteries and the hydrogen energy subsystem are a backup for renewables. Batteries are convenient to use for storing energy, and their life span is dependent on the number of charge/discharge cycles, so their quantity and use frequency should be kept to a minimum [33]. In the paper, batteries should keep some energy to make sure the basic electrical consumption and hydrogen tanks should be restored to the initial state after a season.

2.2. Modeling the System Components

2.2.1. Photovoltaic System

The output power of each PV panel at time t could be obtained from solar radiation by the following equation [34]:

$$p_{PV}(t) = \frac{G(t)}{1000} p_{PV,rated} \times \eta_{PV,conv} \tag{1}$$

where G is the perpendicular insolation at the panel's surface (W/m^2), $p_{PV,rated}$ is the rated power of each PV panel at $G = 1000$ W/m^2 and $\eta_{PV,conv}$ is the efficiency of the PV's DC/DC converter. In this paper, it is assumed that the PV panel has a maximum power point tracking (MPPT) system, which is economical and reasonable, as described in [10,35]. Furthermore, it assumes that the temperature effects are ignored. If the number of PV systems is N_{PV}, the overall produced power is $P_{PV}(t) = N_{PV} \times p_{PV}(t)$.

2.2.2. Wind Turbine Generator

For a wind turbine, the wind speed around is vital. When the wind speed exceeds the cut-in value, the wind turbine generator will start generating. If the wind speed exceeds the rated speed of the wind generator, it generates constant output power, and if the wind speed exceeds the cut-out value, the wind turbine generator stops running to protect the generator [36]. The produced power of each wind generator (p_{WT}) at time t, is obtained as follows:

$$p_{WT}(t) = \begin{cases} 0, & v \leq v_{in} \text{ or } v(t) > v_{out} \\ p_{WT,rated} \times \frac{v(t)-v_{in}}{v_{rated}-v_{in}}, & v_{in} < v(t) \leq v_{rated} \\ p_{WT,rated}, & v_{rated} < v(t) \leq v_{out} \end{cases} \tag{2}$$

where $v(t)$ is the wind speed (m/s) at time t, $p_{WT,rated}$ is the rated power of the wind generator (kW), v_{in}, v_{out} and v_{rated} are cut-in, cut-out and rated speed of wind generator (m/s), respectively. If the number of wind generators is N_{WT}, the overall produced power is $P_{WT}(t) = p_{WT}(t) \times N_{WT}$.

Above all, the energy generated from renewable resources can be expressed as:

$$P_{gen}(t) = P_{PV}(t) \times \eta_{Inv} + P_{WT}(t) \times \eta_{Inv}^2 \tag{3}$$

where η_{Inv} denotes the inverter efficiency.

2.2.3. Battery

The operation states of PV panels and wind generators are completely dependent on the climatic conditions. This causes a great deal of reliability concern. To improve the system reliability and to store the excess energy, batteries are much needed in such hybrid systems. In order to analyze the batteries' performance, usually we use the state of charge (SOC) expressed as Equation (4) to describe energy in the battery [37].

$$SOC = \frac{E_{Bat}(t)}{E_{Bat,cap}} \times 100\% \tag{4}$$

where $E_{Bat}(t)$ is the energy at time t and $E_{Bat,cap}$ is the energy when the battery is fully charged. In order to increase the battery life, it has a limitation as $SOC \in [SOC_{min}, SOC_{max}]$.

When the total output of the PV panels and wind generators is greater than the load demand, the battery will be in the charging state. When the total output of the PV panels and wind generators is less than the load energy, the battery is in the discharging state. The battery energy at time t can be expressed as:

$$E_B(t+1) = E_B(t) \times (1-\sigma) + [E_{gen}(t+1) - \frac{E_L(t+1)}{\eta_{Inv}}] \times \eta_{BC}, \quad E_{gen}(t+1) > \frac{E_L(t+1)}{\eta_{Inv}} \tag{5}$$

$$E_B(t+1) = E_B(t) \times (1-\sigma) - \frac{\frac{E_L(t+1)}{\eta_{Inv}} - E_{gen}(t+1)}{\eta_{Inv}} \times \eta_{BF}, \quad E_{gen}(t+1) < \frac{E_L(t+1)}{\eta_{Inv}} \tag{6}$$

where $E_B(t)$ is the battery energy at time t, σ is the hourly self-discharge rate, $E_L(t)$ is the demand of load at time t and η_{BC} is the charge efficiency of batteries. η_{BF} is the discharging efficiency of batteries, which is assumed to be one in the paper.

Remark 1. *A 1-h time step is employed. Thus, generated and demanded power are equivalent to generated and demand energy in value at a particular hour, as is specified by Equations (7) and (8):*

$$P_{gen}(t) = E_{gen}(t) \tag{7}$$

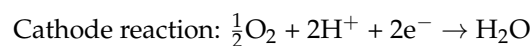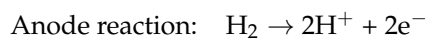$$P_L(t) = E_L(t) \tag{8}$$

2.2.4. Hydrogen Subsystem

Considering the battery capacity limitation, leakage characteristic and high price, when the system still has remaining electrical energy and the batteries are full, the electrolyzer could transfer the remaining energy to hydrogen, so as not to waste too much. Additionally, the power from the electrolyzer to the hydrogen tank can be defined as follows:

$$P_{el-tank}(t) = P_{gen-el}(t) \times \eta_{el} \tag{9}$$

where η_{el} is the electrolyzer efficiency, which is assumed to be constant between zero and one. $P_{el-tank}(t)$ and $P_{gen-el}(t)$ are the transferred power from the electrolyzer to the hydrogen tank and the transferred power from the generated power system to the electrolyzer, respectively.

Some electrical energy could be produced through the FC when there is enough hydrogen. In this work, the proton exchange membrane fuel cell (PEMFC) has been adopted, and its working principle is expressed as follows:

$$\text{Anode reaction:} \quad H_2 \rightarrow 2H^+ + 2e^-$$

$$\text{Cathode reaction:} \quad \tfrac{1}{2}O_2 + 2H^+ + 2e^- \rightarrow H_2O$$

In [38], the hydrogen consumption to 1 kWh electrical energy is 26.8 mol·h^{-1} under the given working conditions. The energy of hydrogen stored in the tank at time step t can be calculated as:

$$E_T(t+1) = E_T(t) + P_{E-T}(t+1) - P_{T-FC}(t+1) \times \eta_{storage} \tag{10}$$

where $E_T(t)$ is the energy stored in the tank at the time t, $P_{T-FC}(t)$ is the power transferred from the hydrogen tank to fuel cells and $\eta_{storage}$ is the corresponding efficiency as a constant.

2.2.5. Direct Current/Alternating Current Converter

Finally, an inverter converts electrical power from DC into AC form at the desired frequency of load. The inverter's losses can be presented by the inverter's efficiency (η_{Inv}).

$$P_{Inv-L}(t) = (P_{FC-Inv}(t) + P_{gen-Inv}(t) + P_{B-Inv}(t)) \times \eta_{Inv} \tag{11}$$

where $P_{gen-Inv}(t)$, $P_{FC-Inv}(t)$ and $P_{B-Inv}(t)$ are the energy transferred from the generation unit, fuel cell and battery at time t, respectively. $P_{Inv-L}(t)$ is the total energy injected into the load at time t.

3. Objectives and Operation Strategy

The objective functions of the optimal sizing problem are the minimization of the annual system cost (C_{total}) and the LPSP. A suitable operation strategy could make each component function properly as much as possible.

3.1. Objective Modelings

3.1.1. Annual System Cost

In this optimal sizing problem, the total annual system cost includes DEC, EWC and HPC, seen in Figure 2. As similar as other studies, DEC is composed of investment, operation and maintenance (O&M) and replacement costs, defined by:

$$C_{DEC} = (C_{INV} + C_{O\&M} + C_{REP})/T_{Sys} \tag{12}$$

- Investment cost:

$$C_{INV} = C_{PV} \times N_{PV} + C_{WG} \times N_{WG} + C_{Bat} + C_{EL} + C_{FC} + C_{HY} \times N_{HY} + C_{Inv} \tag{13}$$

　　where C_{PV}, C_{WG}, C_{Bat}, C_{EL}, C_{FC}, C_{HY} and C_{Inv} are the price of the PV, wind turbine, battery, electrolyzer, FC, hydrogen tank and inverter, respectively. N_x is the number of component x.
- O&M cost:

$$C_{O\&M} = \alpha \times C_{INV} \times T_{Sys} \tag{14}$$

　　where α is a coefficient. Additionally, we defined the operating time of the hybrid system (T_{Sys}) as 20 years, because the PV panel has the longest lifetime (about 20 years) among all of the components.
- Replacement cost:

$$
\begin{aligned}
C_{REP} = & C_{Bat} \times N_{Bat} \times \sum_{n}^{T_{Sys}/T_{Bat}} \frac{1}{(1+i)^{n \times T_{Bat}}} \\
& + C_{EL} \times N_{EL} \times \sum_{n}^{T_{Sys}/T_{EL}} \frac{1}{(1+i)^{n \times T_{EL}}} \\
& + C_{FC} \times N_{FC} \times \sum_{n}^{T_{Sys}/T_{FC}} \frac{1}{(1+i)^{n \times T_{FC}}}
\end{aligned}
\tag{15}
$$

where i is the interest rate and T_{Bat} (two years), T_{EL} (five years) and T_{FC} (five years) are the lifetime of the battery, electrolyzer and FC, respectively. This means that in this hybrid system, the battery, electrolyzer and FC should be replaced according to the schedule.
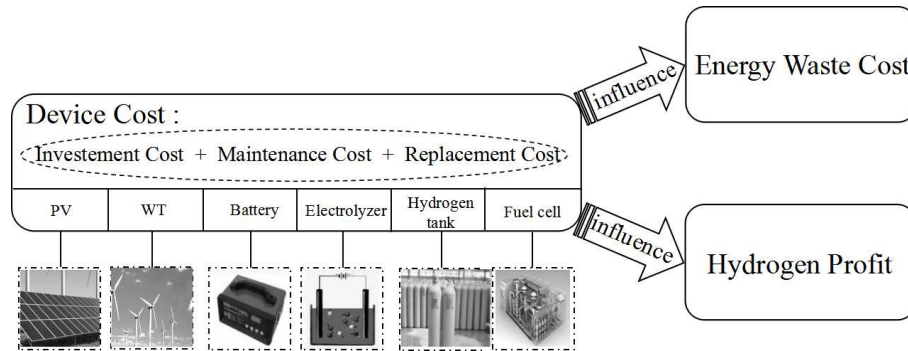

Figure 2. The model of the annual system cost.

Although there are battery and hydrogen subsystems to store excess energy, still, some energy may be wasted when they are full. In this case, we could use EWC to measure the waste as the following equation:

$$C_{EWC} = \sum \frac{C_{DEC}}{E_{out\_annual}} \times (P_{gen}(t) - P_L(t) - P_{stor}(t)) \tag{16}$$

where E_{out_annual} is the average output of the generation unit every year and $P_{gen}(t)$, $P_L(t)$ and $P_{stor}(t)$ are the energy generated, consumed and stored at time t, respectively.

In order to utilize the hydrogen subsystem reasonably, we could check the status of the hydrogen tanks and let them restore the initial level at the end of each season. HPC could be obtained by:

$$C_{HPC} = \sum \frac{C_{DEC}}{E_{out\_annual}} \times \frac{E_{HY}(i)}{\eta_{el}} \tag{17}$$

where $E_{HY}(i)$ is the energy stored in hydrogen tanks at the end of each season. Obviously, HPC is useful to decrease the total cost.

Above all, the annual system cost (C_{total}) is the sum of DEC, EWC and HPC expressed by the following equation:

$$C_{total} = C_{DEC} + C_{EWC} - C_{HPC} \tag{18}$$

3.1.2. Reliability

Due to the unpredictable nature of the power produced by PV and the wind generator, an analysis for the reliability plays a vital role for a hybrid system design. When $P_{avai}(t) < P_L(t)$, the reliability analysis is significant. There are various methods for carrying out the reliability analysis: the LPSP, defined as Equation (19), is one of the widely-used methodologies for this purpose.

$$LPSP = \frac{\sum Time(if\, P_{avai}(t) < P_L(t))}{T} \tag{19}$$

where T is the number of hours in the study and $P_{avai}(t)$ can be described as Equation (20).

$$P_{avai}(t) = P_{PV}(t) + P_{WT}(t) + P_{Bat}(t) + P_{HY}(t) \tag{20}$$

If a system in the electrical field has insufficient power to feed the load demand, i.e., has a small LPSP, it is regarded as a reliable system. A LPSP of zero means that the load demand is absolutely satisfied; and a LPSP of one means that the power generated does not meet the demand of the load.

Additionally, in order to make certain the basic electricity consumption because of lighting and water drinking, see [39]. It is essential to keep the initial energy in the batteries after 24 h (Figure 3).
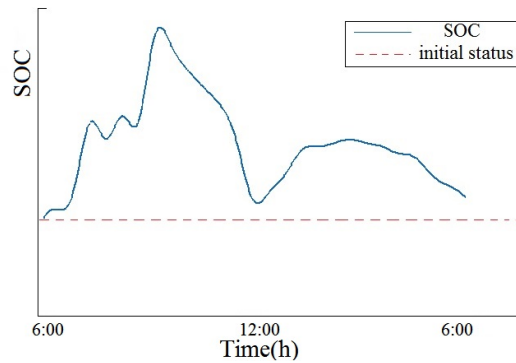

Figure 3. Initial status of the battery.

3.2. Constraints

For the hybrid power system, the following constraints should be satisfied:

$$N_{PV} = Integer, \ \ 0 < N_{PV} < N_{PV}^{max} \tag{21}$$

$$N_{WG} = Integer, \ \ 0 < N_{WG} < N_{WG}^{max} \tag{22}$$

$$N_{Bat} = Integer, \ \ 0 < N_{Bat} < N_{Bat}^{max} \tag{23}$$

$$N_{HY} = Integer, \ \ 0 < N_{HY} < N_{HY}^{max} \tag{24}$$

where N_{PV}^{max}, N_{WG}^{max}, N_{Bat}^{max} and N_{HY}^{max} are the maximum available number of PV panels, wind turbines, batteries and hydrogen tanks, respectively.

Summary: From the above description, the mathematical model of this sizing problem in HS-BH could be expressed as follows:

$$
\begin{aligned}
\min C_{total} &= C_{DEC} + C_{EWC} - C_{HPC} \\
s.t. \ \ LPSP &\leq 0.1\% \\
N_x &\in (0, N_x^{max}]
\end{aligned}
\tag{25}
$$

where N_x represents N_{PV}, N_{WG}, N_{Bat} and N_{HY}, respectively. According to some restrictions on economy and reliability, the numbers of components in HS-BH could be ensured.

3.3. Operation Strategy

In this paper, the hybrid energy system operates as the following strategy:

- If $P_{gen}(t) = P_L(t) / \eta_{Inv}$, this means that the whole power generated by renewable sources (solar and wind) is injected to the load through the inverter (like the other Step 1 in Figure 4).
- If $P_{gen}(t) > P_L(t) / \eta_{Inv}$, this means that there will be some remaining electrical energy, which would not be injected. In this case, $SOC(t)$ will be judged, so as to decide where the remaining energy goes.
  If $SOC(t) < SOC_{max}$, the surplus power is transferred to batteries till the SOC equals SOC_{max} or there is no surplus power. If $SOC(t) = SOC_{max}$, the electrolyzer should work for transferring the surplus power to hydrogen till there is no surplus power and then goes to the other Step 2 in Figure 4.
- If $P_{gen}(t) < P_L(t) / \eta_{Inv}$, this means that the energy generated is not enough to supply the load demand. In this case, the storage system (battery and hydrogen subsystem) will work so as to

achieve a balance. Furthermore, $SOC(t)$ will be judged so as to decide the procedure between the two storage subsystems.

If $SOC(t) > SOC_{min}$, the shortage power will be supplied by batteries till the SOC equals SOC_{min}. If $SOC(t) = SOC_{min}$, the batteries could not discharge any more. The fuel cells will be started to supply the load and then goes to the other Step 2 in Figure 4. Additionally, if the shortage power exceeds the fuel cell's rated power or stored hydrogen cannot afford the shortage, some fraction of the load must be shed. This fact leads to a loss of load.
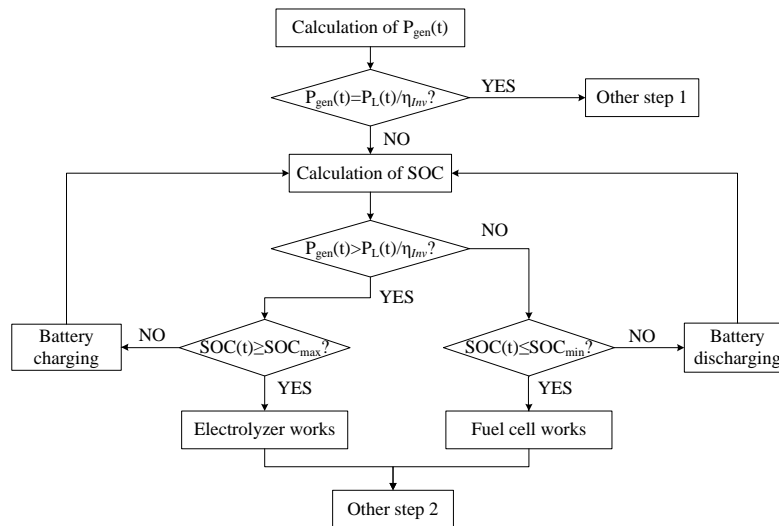
Figure 4. Operation strategy of the hybrid system.

4. Improved Ant Colony Optimization Algorithm

Due to the complexity of the optimal sizing problem of the considered hybrid system, classical optimization methods have failed to be either effective or efficient. Meta-heuristics are designed to tackle complex optimization problems. Ant colony algorithm is selected in this study because of its advantages.

4.1. Ant Colony Optimization Basics

Dorigo [40] proposed an intelligent optimization algorithm named ant colony algorithm (ACO), which is based on the ant's behavior in nature.

In the initial stage, ACO is mainly used to solve the traveling salesman problem (TSP), which is a famous problem in the mathematics field. Each ant in the node *i* moves to the next node *j* (selected among the unvisited cities) according to a certain probability, so as to obtain the minimum distance from start node to the destination. The probability is calculated according to the pheromone:

$$p_{ij}^{k} = \frac{[\tau_{ij}(t)]^{\alpha} \times [\eta_{ij}(t)]^{\beta}}{\sum_{s \in J_k(i)} [\tau_{is}(t)]^{\alpha} \times [\eta_{is}(t)]^{\beta}} \tag{26}$$

where $\tau_{ij}(t)$ is the pheromone between *i* and *j* at time *t*, $\eta_{ij}(t)$ is the heuristic factor and α and β are the coefficients, which stand for the importance degree of τ and η, respectively. $J_k(i)$ is the set consisting of the cities that ant *k* could select. Ants in ACO could communicate and cooperate easily with each other. Ant colony algorithm has strong robustness and the concurrency of the search process. The ant colony algorithm is not dependent on the selection of an initial route and does not need manual intervention [41].

However, when the problem has a larger scale, the time for searching the result using ACO will be too much. It is hard to highlight the advantages of ACO at the beginning.

4.2. Improved Ant Colony OptimizationAlgorithm

In order to shorten the ACO search time, we could highlight some routes that are relatively optimal at the current time in some way. In this case, ants will tend to select among the routes highlighted, while not selecting among all of the possible routes. Therefore, ants could select several better routes easily based on Equation (26).

Based on the above idea, we could modify the rules of updating the pheromone. In each iteration, we calculate the system cost of every ant and then sort the corresponding routes and ants according the system cost in ascending order (an ant has a route). When updating the pheromone, not all of the ants should release pheromone. The amount of pheromone released is proportional to the sequence. At this time, we could set the number of ants (assume *m* ants) that should release pheromone according to the demands. It is noted that *m* should not be too big and too small, for too big *m* (here, *m* is 10) could shorten the search time and too small *m* will increase the probability to fall into local optimal solutions.

In any iteration, the amount of pheromone released by *m* ants could be expressed by the following Equation (27):

$$\tau_{ij}(t+1) = \tau_{ij}(t) + \Delta\tau_{ij}(t) + \Delta\tau_{ij}^*(t) \tag{27}$$

$$\Delta\tau_{ij}(t) = \sum_{r=1}^{m} \frac{Q}{L^r(t)} \tag{28}$$

where Q is a constant, $L_r(t)$ is the system cost of ant r and if the ant r moved from i to j, the ant r will release pheromone like Equation (28), or $\Delta\tau_{ij}(t)$ will be zero.

If the best ant, i.e., the first ant in the sequence, moved from i to j, it will release extra pheromone like Equation (29), or $\Delta\tau_{ij}^*(t)$ will be zero.

$$\Delta\tau_{ij}^*(t) = \frac{Q}{L^*(t)} \tag{29}$$

Compared with the general ACO using the experiment dataset named eil51 [42] adopted from a well-known electronic library TSPLIB, the advantage of the improved ACO could be seen clearly in Figure 5. Its convergence effect and the best solution are more outstanding.
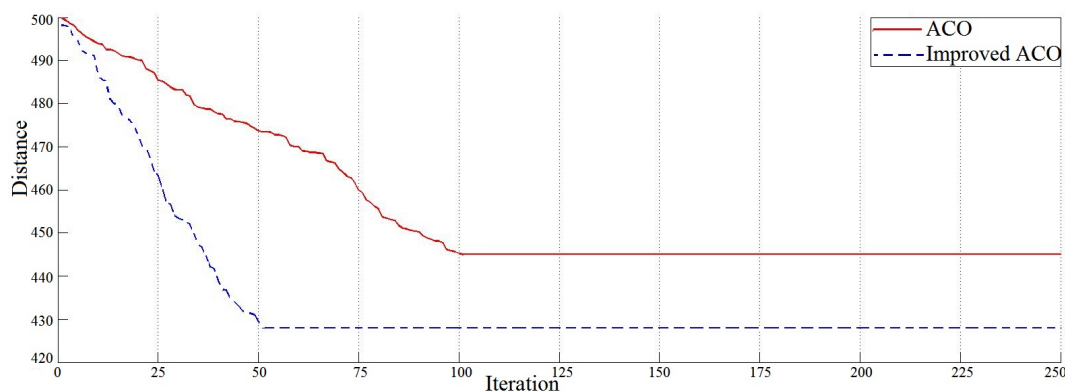

Figure 5. The result of the eil51 simulation.

5. Result and Analysis

5.1. Simulation Result

In this paper, an improved ACO based on a real encoding and sorting mechanism is adopted to optimize the number of system components (we call these numbers variables). What is different from TSP, the amount of pheromone released is not based on the length of the route, but the corresponding system cost, i.e., the amount of pheromone is inversely proportional to the system cost. As required,

there will be 12 bits when we set each variable to have three bits, and each bit ranges from zero to nine. Therefore, every bit represents a node, and between two bits, there are 10 paths, as in Figure 6.
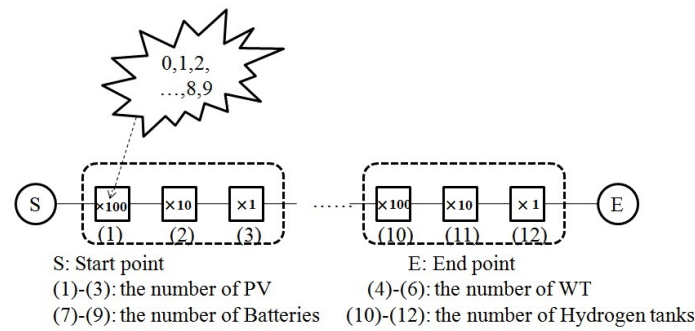

Figure 6. Encoding representation.

At first, all of the ants are at the start point S in Figure 6, then they will search the best route, as the following steps seen Figure 7.
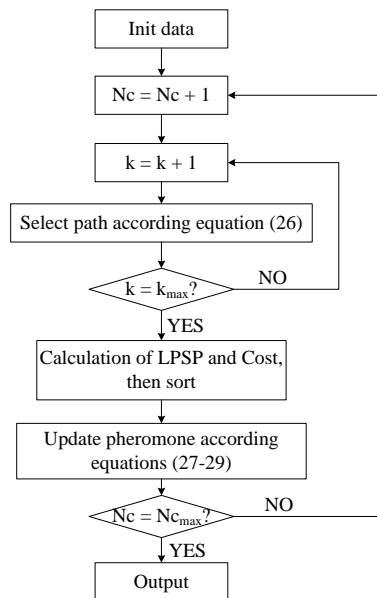

Figure 7. Algorithm flow.

(1) Initialize the amount of pheromone between every two bits, and set the iterations N_{Cmax}, the maximum number of ants k_{max}, the number of ants needed to be sorted *m*, the constant *Q* and other important parameters.

(2) Increase the current iteration $N_c = N_c + 1$.

(3) Count the ant $k = k + 1$. In each iteration, all of the ants will search routes one by one.

(4) Each ant selects a path among 10 available paths so as to get the next bit according to the probability described as Equation (26) till achieving the end point.

(5) Judge the relation between the current *k* and k_{max}. If $k < k_{max}$, turn to Step (3) or turn to Step (6).

(6) Calculate the system cost and LPSP of ant *k*. Additionally, find the ants whose LPSP is not more than the given LPSP; sort them according to the system cost; then select the *m* ants (here, m is 10) we needed.

(7) Update the pheromone as described in Equation (27).

(8) Judge the relation between the current N_c and N_{Cmax}. If $N_c < N_{Cmax}$, turn to Step (2) or turn to Step (9).

(9) Output the data demanded and draw the figures.

The simulation data, including average irradiation around the year, average wind speed around the year (Table 1) and daily load (Figure 8), are produced with the reference of that gained from an island in Zhoushan, Zhejiang, China, in summer 2015. Figure 9 is the data measured one day in July 2015. In this study, the minimum and maximum bounds of the decision variables are set to zero and 200 for the PV panels and wind turbines and set to zero and 900 for the batteries and hydrogen tanks. At the initial moment, it is assumed that the charge of each battery is 30% of its nominal capacity.

Table 1. Average wind speed and irradiation.

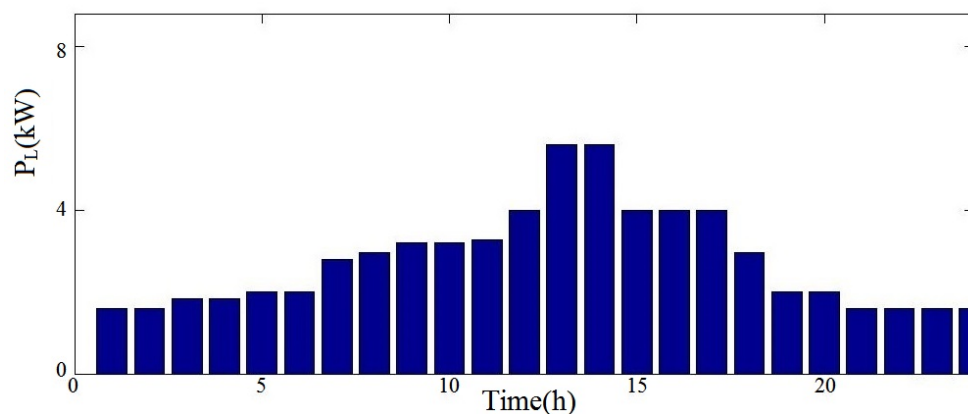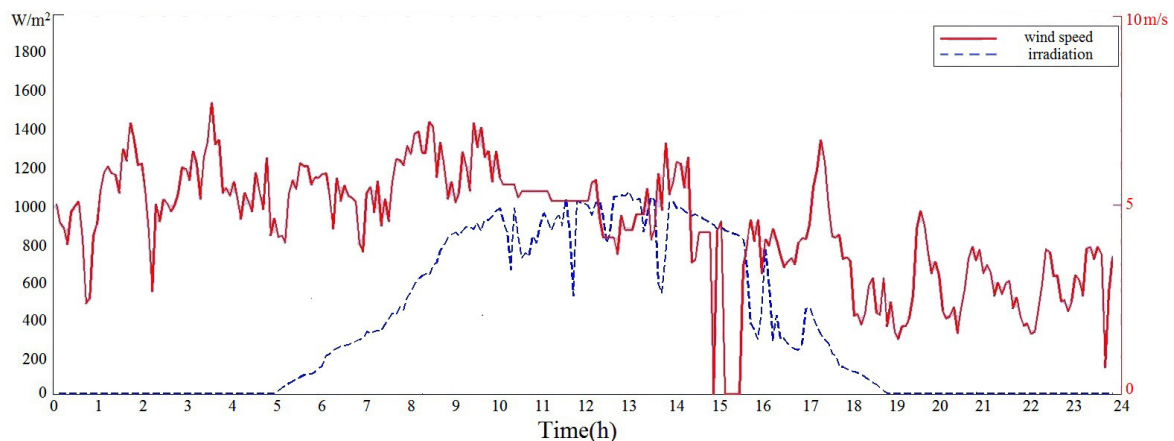| Month	Wind Speed (m/s)	Irradiation (kW/m^2)
January	7.41	15
February	7.28	18
March	5.85	20
April	5.20	30
May	4.81	45
June	4.94	53
July	4.55	50
August	4.42	51
September	5.85	50
October	6.76	43
November	7.54	38
December	8.19	20

Figure 8. Daily load.

Figure 9. One day irradiation in July.

Here is some pseudocode of the improved ACO.

THE IMPROVED ACO

1 ▷ Initialization for several parameters such as N_{Cmax}, k_{max}, m, Q, etc.
2 $k \leftarrow 1$
3 $N_{Cmax} \leftarrow 1$
4 **while** $N_c < N_{Cmax}$
5   **do** $N_c \leftarrow N_c + 1$
6   **while** $k < k_{max}$
7   **do** $k \leftarrow k + 1$
8   **while** $j < 12$
9   **do**
10   **while** $i < 10$
11   **do** $p \leftarrow \frac{[\tau_{ij}(t)]^\alpha \times [\eta_{ij}(t)]^\beta}{\sum_{s \in J_k(i)} [\tau_{is}(t)]^\alpha \times [\eta_{is}(t)]^\beta}$ ▷ this is Equation (26)
12   select the node d whose probability (p) is maximum
13   get the route of ant k according the selected nodes above
14   ▷ calculate the LPSP and total cost of the route
15                     $LPSP \leftarrow \frac{\sum Time(if P_{avai}(t) < P_L(t))}{T}$ ▷ this is Equation (19)
16                     $C_{total} \leftarrow C_{DEC} + C_{EWC} - C_{HPC}$ ▷ this is Equation (18)
17   select the routes based on the demand of LPSP and sort them based on the C_{total}
18   select m routes
19                 $\tau_{ij}(t+1) \leftarrow \tau_{ij}(t) + \Delta\tau_{ij}(t) + \Delta\tau_{ij}^*(t)$ ▷ this is Equation (27)

The hybrid solar-wind system usually meets the load demands well because of the good complementary effect of the solar radiation and wind speed. The optimal sizing result for the LPSP of 0.01 is shown in Table 2 and in Figure 10.

Table 2. Simulation result.

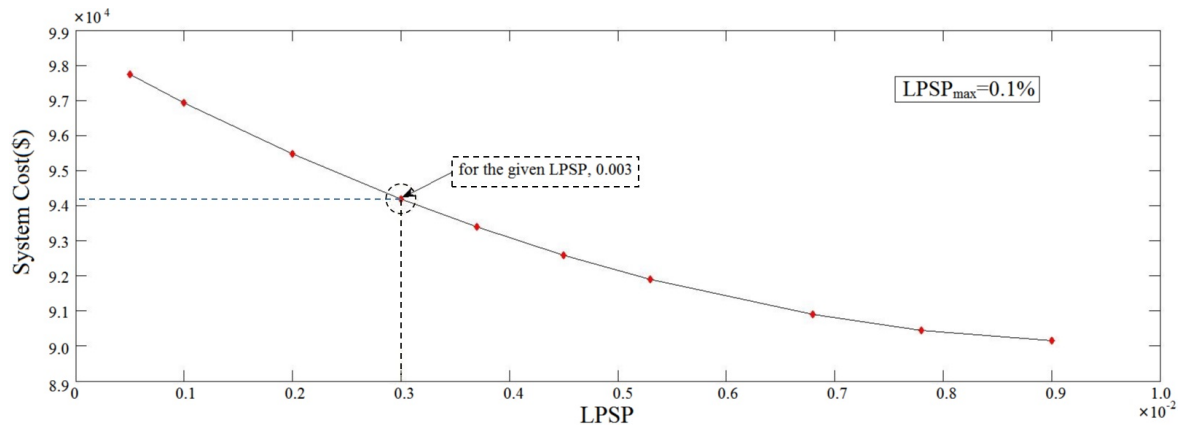| Cost ($\times 10^4$)	LPSP ($\times 10^{-2}$)	N_{PV}	N_{WT}	N_{bat}	$N_{Hydrogen}$
8.99	0.90	90	9	232	307
9.06	0.78	92	11	240	307
9.13	0.68	95	11	243	309
9.18	0.53	99	12	253	311
9.21	0.45	107	13	267	313
9.39	0.37	113	15	271	313
9.41	0.30	120	14	272	315
9.53	0.20	130	16	283	327
9.64	0.10	143	16	287	329
9.83	0.05	147	17	292	331

Figure 10. Simulation result for different LPSP.

5.2. Analysis

The program optimizes both the system cost and LPSP. From the result in Figure 10, it is obvious that decreasing the system cost and increasing the system reliability are paradoxical. If we want to make the system more reliable, more system cost should be put into it.

Since the hybrid system is civilian, an excellent LPSP system is too expensive for residents. Furthermore, a too high LPSP system will influence residents' lives. Therefore, when N_{PV} = 120, N_{WT} = 14, N_{Bat} = 272, N_{H_2} = 315, the system could be built and operated with a low cost in the case of the given LPSP. Here, C_{total} = 9.41×10^4, LPSP = 0.003.

Additionally, for this LPSP, the energy stored in the battery in one year is shown in Figure 11, and the hydrogen stored in tanks at the end of each season is zero for spring, 2000 kWh for summer, 1103 kWh for autumn and zero for winter. As a result, DEC has 103% in annual system cost (9.41 × 10^4); EWC has 5%; and HPC has 8% (HPC is profit, which could reduce the annual system cost).
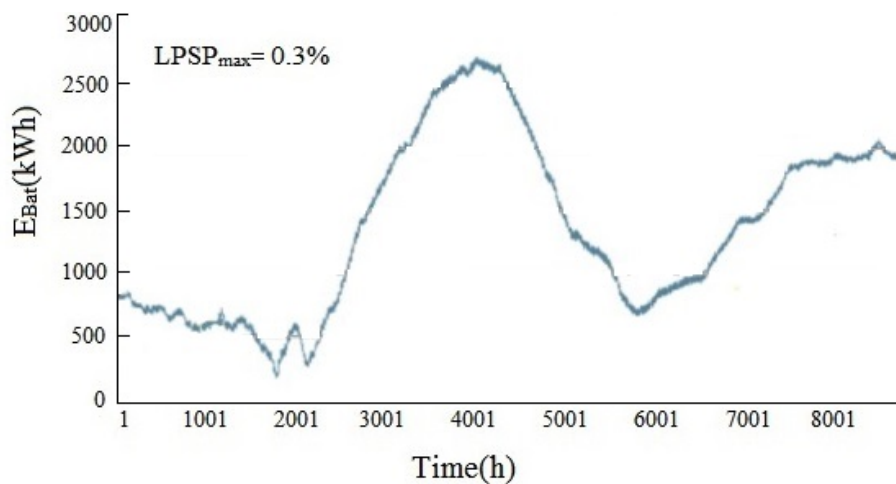

Figure 11. Energy in batteries.

Moreover, comparative simulations have been finished for emphasizing the advance of the proposed hybrid system when LPSP = 0.03. Two extra power systems, including the battery-based hybrid system and the FC-based hybrid system, are adopted. From the comparisons, it is easy to analyze the total DEC of these three systems and the corresponding breakdown, that is to say, the proportion of each component in total DEC.

As seen in Figure 12a–c, under the premise of satisfying reliability, the minimum total cost is USD96,923, USD97,867 and USD102,366, respectively. Because of the battery leakage, only if there

are enough batteries could the battery-based hybrid system maintain power supply requirements in a long lifetime (20 years). In the FC-based hybrid system, the fuel cells' leakage ratio is nearly zero, which could be ignored. However, the efficiency of FC is less than the battery; only if there are enough renewable resources and hydrogen tanks could this system satisfy LPSP.
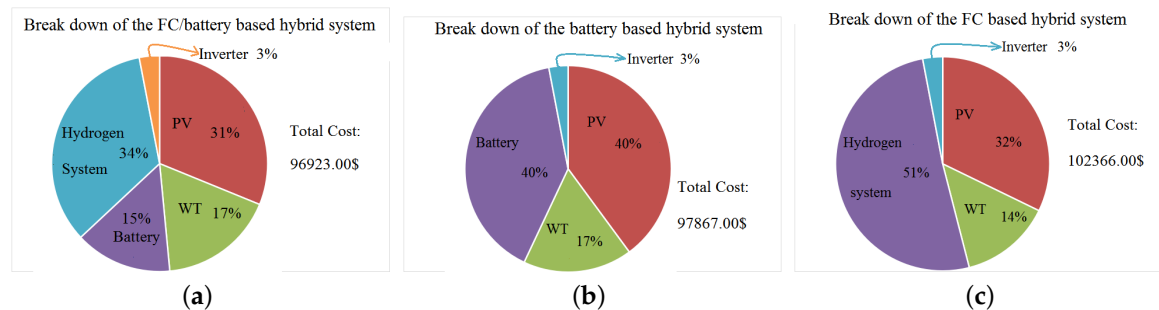

Figure 12. Comparison of three kinds of hybrid power systems. (**a**) Breakdown of the fuel cell (FC)/battery-based hybrid system; (**b**) breakdown of the battery-based hybrid system; and (**c**) breakdown of the FC-based hybrid system.

6. Conclusions and Outlook

In the paper, we introduced the components of the PV/WT/battery/hydrogen hybrid system and the energy relation among them. As two storage subsystems (the battery and hydrogen storage subsystem) were added, the hybrid system was more complicated than usual. According to the actual data gained from an island in Zhoushan, Zhejiang, China, in summer 2015, the detailed annual system cost (consisting of DEC, EWC and HPC) calculation method and the grading method were introduced. In order to realize the goal efficiently, an improved ACO based on sorting, which could help to shorten the search time, was used. At last, we find that decreasing the system cost and increasing the system reliability are paradoxical. For a given LPSP, a suitable sizing has been chosen from the simulation result, which is described in Figure 10.

The comparison simulations among the hybrid system in this paper, the battery-based hybrid system and the FC-based hybrid system have been conducted. Due to the battery leakage and the FC lower efficiency, under certain constraints, the hybrid system proposed in this paper is more economical than others.

Although such heuristic algorithms could give the global optimal solution for NP problems, the accuracy could not be guaranteed completely within a reasonable amount of time all of the time. Some more work should to be done in the future. For example, with respect to the problem description, the data used in this study may not be enough, and we should measure more typical data; many factors in the models should be considered when analyzing the models, so as to be more accurate; on the other hand, in the improved ACO, the number of ants selected (m) is very important to this study and could now be determined just by trail and error. Additionally, the storage strategy is certainly simple in our current work. As presented in [43], the energy storage strategy is vital to stand-alone photovoltaic power systems. A more comprehensive storage strategy is significant for HS-HB, and this is what we should focus on next.

Author Contributions: Weiqiang Dong, Yanjun Li and Ji Xiang conceived and designed the experiments; Weiqiang Dong performed the experiments; Weiqiang Dong and Yanjun Li analyzed the data; Ji Xiang contributed experiment data; Weiqiang Dong wrote the paper.

Conflicts of Interest: The authors declare no conflict of interest.

References

1. Wu, K.; Zhou, H.; An, S.; Huang, T. Optimal coordinate operation control for wind photovoltaic battery storage power-generation units. *Energy Convers. Manag.* **2015**, *90*, 466–475.
2. Mahesh, A.; Sandhu, K.S. Hybrid wind/photovoltaic energy system developments: Critical review and findings. *Renew. Sustain. Energy Rev.* **2015**, *52*, 1135–1147.
3. Lin, W.M.; Lu, K.H.; Ou, T.C. Design of a novel intelligent damping controller for unified power flow controller in power system connected offshore power applications. *IET Gener. Transm. Distrib.* **2015**, *9*, 1708–1717.
4. Ou, T.C. A novel unsymmetrical faults analysis for microgrid distribution systems. *Int. J. Electr. Power Energy Syst.* **2012**, *43*, 1017–1024.
5. Ou, T.C. Ground fault current analysis with a direct building algorithm for microgrid distribution. *Int. J. Electr. Power Energy Syst.* **2013**, *53*, 867–875.
6. Belfkira, R.; Zhang, L. Optimal sizing study of hybrid wind/PV/diesel power generation unit. *Sol. Energy* **2011**, *85*, 100–110.
7. Kellogg, W.D.; Nehrir, M.H. Generation unit sizing and cost analysis for stand-alone wind, photovoltaic, and hybrid wind/PV systems. *IEEE Trans. Energy Convers.* **1998**, *13*, 70–75.
8. Li, J.; Wei, W.; Xiang, J. A Simple Sizing Algorithm for Stand-Alone PV/Wind/Battery Hybrid Microgrids. *Energies* **2012**, *5*, 5307–5323.
9. Akella, A.K.; Sharma, M.P. Optimum utilization of renewable energy sources in a remote area. *Renew. Sustain. Energy Rev.* **2007**, *11*, 894–908.
10. Elbaset, A.A. Design, Modeling and Control Strategy of PV/FC Hybrid Power System. *Electr. Syst.* **2011**, *7*, 270–286.
11. Vafaei, M. Optimally-Sized Design of a Wind/diesel/fuel Cell Hybrid System for Remote Community. Master's Thesis, University of Waterloo, Waterloo, ON, Canada, 2011.
12. Herrera, V.; Milo, A. Adaptive energy management strategy and optimal sizing applied on a battery-supercapacitor based tramway. *Appl. Energy* **2016**, *169*, 831–845.
13. Abdin, Z.; Webb, C.J. Solar hydrogen hybrid energy systems for off-grid electricity supply: A critical review. *Renew. Sustain. Energy Rev.* **2015**, *52*, 1791–1808.
14. Kaviani, A.K.; Baghaee, H.R. Optimal sizing of a stand-alone Wind/Photovoltaic generation unit using particle swarm optimization. *Simulation* **2009**, *85*, 89–99.
15. Kaviani, A.K.; Riahy, G.H. Optimal design of a reliable hydrogen-based stand-alone wind/PV generation system, considering component outages. In Proceedings of the 11th International Conference on Optimization of Electrical and Electronic Equipment, Brasov, Romania, 22–24 May 2008; pp. 413–418.
16. Torreglosa, J.P.; Garcia, P. Energy dispatching based on predictive controller of an off-grid wind turbine/photovoltaic/hydrogen/battery hybrid system. *Renew. Energy* **2015**, *74*, 326–336.
17. Gong, Q.; Lei, J. Optimal siting and sizing of distributed generators in distribution systems considering cost of operation risk. *Energies* **2016**, *9*, 61, doi:10.3390/en9010061.
18. Kara, O. Optimization of a wind/PV hybrid power generation system. *Int. J. Green Energy* **2005**, *2*, 57–63.
19. Kuznia, L.; Bo, Z.; Centeno, G.; Miao, Z. Stochastic optimization for power system configuration with renewable energy in remote areas. *Ann. Oper. Res.* **2013**, *210*, 411–432.
20. Malheiro, A.; Castro, P.M. Integrated sizing and scheduling of wind/PV/diesel/battery isolated systems. *Renew. Energy* **2015**, *83*, 646–657.
21. Sunanda, S.; Chandel, S.S. Review of recent trends in optimizaion techniques for solar photovoltaic-wind based energy systems. *Renew. Sustain. Energy Rev.* **2015**, *50*, 755–769.
22. Koutroulis, E.; Kolokotsa, D. Mehtodology for optimal sizing of stand-alone PV/wind-generator systems using genertic algorithms. *Sol. Energy* **2006**, *80*, 1072–1088.
23. Shahirinia, A.H.; Moghaddas-Tafreshi, S.M.; Gastaj, A.H.; Moghaddomjoo, A.R. Optimal sizing of hybrid power system using genetic algorithm. In Proceedings of the 2005 International Conference on Future Power Systems, Amsterdam, The Netherlands, 16–18 November 2005.

24. Xu, D.; Kang, L.; Chang, L.; Cao, B. Optimal sizing of stand-alone hybrid wind/PV power systems using genetic algorithm. In Proceedings of the Canadian Conference on Electrical and Computer Engineering, Saskatoon, SK, Canada, 1–4 May 2005; pp. 1722–1725.

25. Bai, Q. Analysis of particle swarm optimization algorithm. *Comput. Inf. Sci.* **2010**, *3*, 180–184.

26. Biswas, I.; Dash, V.; Bajpai, P. Sizing optimization of PV-FC-Battery system with hybrid PSO-EO algorithm. In Proceedings of the 2012 Annual IEEE India Conference, Kochi, India, 7–9 December 2012; pp. 869–874.

27. Ou, T.C.; Hong, C.M. Dynamic operation and control of microgrid hybrid power systems. *Energy* **2014**, *66*, 314–323.

28. Sharafi, M.; Elmekkawy, T.Y. Multi-objective optimal design of hybrid renewable energy systems using PSO-simulation based approach. *Renew. Energy* **2014**, *68*, 67–79.

29. Ou, T.C.; Chuang, S.J.; Hong, C.M.; Wu, R.C.; Tsao, T.P.; Chen, C.Y. Self-regulation ground faults model for microgrid distribution. *ICIC Express Lett. Part B Appl.* **2015**, *6*, 3225–3230.

30. Wang, W.Y. Routing selection algorithm under multiple link state limited. *J. Comput. Appl.* **2007**, *27*, 2395–2397.

31. Luo, D.L.; Wu, S.-X. Ant colony optimization with potential field heuristic for roboot path planning. *Syst. Eng. Electron.* **2010**, *32*, 1277–1280.

32. Carpaneto, E.; Chicco, G. Ant-colony search-based minimum losses reconfiguration of distribution systems. In Proceedings of the 2004 12th IEEE Mediterranean Electrotechnical Conference, Dubrovnik, Croatia, 12–15 May 2004; pp. 971–974.

33. Dufo-Lopez, R.; Bernal-Agustin, J.L. Optimaization of control straregies for stand-alone renewable energy syatems with hydrogen storage. *Renew. Energy* **2007**, *32*, 1102–1126.

34. Maleki, A.; Pourfayaz, F. Optimal sizing of autonomous hybrid photovoltaic/wind/battery power system with LPSP technology by using evolutionary algorithms. *Sol. Energy* **2015**, *115*, 471–483.

35. Aryani, D.R.; Song, H. Coordination Control Strategy for AC/DC Hybrid Microgrids in Stand-Alone Mode. *Energies* **2016**, *9*, 469, doi:10.3390/en9060469.

36. Garcia, R.S.; Weisser, D. A wind-diesel system with hydrogen storage: Joint optimisation of design and dispatch. *Renew. Energy* **2006**, *31*, 2296–2320.

37. Hong, C.M.; Ou, T.C.; Lu, K.H. Development of intelligent MPPT (maximum power point tracking) control for a grid-connected hybrid power generation system. *Energy* **2013**, *50*, 270–279.

38. Kriston, A.; Szabó, T.; Inzelt, G. The marriage of car sharing and hydrogen economy: A possible solution to the main problems of urban living. *Int. J. Hydrog. Energy* **2010**, *35*, 12697–12708.

39. Iglesias, F.; Palensky, P.; Cantos, S.; Kupzog, F. Demand Side Management for Stand-Alone Hybrid Power Systems Based on Load Identification. *Energies* **2012**, *5*, 4517–4532.

40. Dorigo, M.; Maniezzo, V. Ant system: Optimization by a colony of cooperating agents. *IEEE Trans. Syst.* **1996**, *26*, 29–41.

41. Han, P. *The Theory and Application of Intelligent Control*; China Electric Power Press: Beijing, China, 2012; pp. 39–73.

42. Aziz, O.; Belaid, A. Discrete cuckoo search algorithm for the traveling salesman problem. *Neural Comput. Appl.* **2014**, *24*, 1659–1669.

43. Li, C.H.; Zhu, X.J. Dynamic modeling and sizing optimization of stand-alone photovoltaic power systems using hybrid energy storage technology. *Renew. Energy* **2009**, *34*, 825–826.